Relation between interface roughness and giant magnetoresistance in MBE-grown polycrystalline Fe/Cr superlattices

P. Beliën, R. Schad, C. D. Potter, G. Verbanck, V. V. Moshchalkov, and Y. Bruynseraede
Laboratorium voor Vaste-Stoffysika en Magnetisme, Katholieke Universiteit Leuven, Celestijnenlaan 200 D, B-3001 Leuven, Belgium
(Received 20 June 1994)

We have studied the influence of the interface roughness on the giant magnetoresistance (GMR) of polycrystalline Fe/Cr superlattices, grown by molecular beam epitaxy on polycrystalline substrates. The interface quality was changed systematically by varying the growth temperature between 0 and 400 °C and by the use of a Cr seed layer. X-ray-diffraction spectra, combined with resistivity data, show that a moderate step density at the interfaces can enhance the GMR, whereas interdiffusion and important interface roughness strongly suppress the GMR.

Since the discovery of the magnetic exchange coupling of ferromagnetic layers across nonmagnetic spacer layers[1,2] and the associated giant magnetoresistance (GMR) effect,[3] three major facts have been well established. First, the GMR is due to the asymmetry in scattering probability for spin-up and spin-down conduction electrons,[4] which drastically decreases the resistivity when an external magnetic field aligns all magnetic moments. Second, impurity atoms in or next to the magnetic host material can enhance the GMR effect.[4,5] Third, the strength of the exchange coupling,[6] as well as the magnitude of the GMR (Refs. 7 and 8) are nonmonotonously decreasing as a function of the spacer layer thickness. Since the scattering asymmetry for spin-up and spin-down electrons is drastically enhanced when an impurity atom from the spacer layer enters the ferromagnetic host matrix, most of the spin-dependent scattering events occur at the interface. Therefore, the properties of the interface are of major importance. Numerous observations have been reported, indicating that interface roughness plays a crucial role in the GMR effect.[4,5,9–16] However, no clear picture has yet emerged and the reported data are apparently contradictory.

Theoretically, it was shown[15,16] that perfect interfaces will not contribute to the GMR. Some models assume the magnitude of the GMR to increase with increasing interface roughness,[15] while other calculations show the existence of an optimal interface roughness.[16]

From the experimental point of view, it was shown that the presence of so-called "asymmetric" scattering centers in the magnetic host is essential in order to increase the difference in scattering probabilities for conduction electrons with different spin orientations.[5] This suggests that some kind of roughness at the interface is needed to observe the GMR effect. Petroff *et al.*[4] reported an increase in the GMR for molecular beam epitaxy (MBE)-grown epitaxial Fe/Cr superlattices with moderate interface roughness. Further increase of the interface roughness, by artificial intermixing, leads to a lower GMR, thus suggesting that an optimum degree of interface roughness is needed. Unfortunately, in these experiments, the Fe and Cr thicknesses were also varied which may have influenced the GMR as well. Fullerton *et al.*[13] showed that in textured Fe/Cr multilayers prepared by sputtering, an increase of the GMR effect is related to roughening of the layers (rather than to interdiffusion). Contrary to this, Takanashi *et al.*[9] studied the GMR of polycrystalline, sputtered Fe/Cr superlattices as function of the lattice parameter at the interface and showed that a reduced lattice spacing spread at the interface enhances the GMR. A similar observation was reported by Rensing, Payne, and Clemens[11] and Joo *et al.*,[12] who showed that smoother interfaces are necessary in order to increase the GMR in Fe/Cr multilayers. Parkin[10] correlated, for sputtered Fe/Cr multilayers, the GMR with the width of the high-angle x-ray-diffraction (HAXRD) FeCr peak which provides information about the crystalline coherence length in the superlattice. He concluded that an increasing coherence length corresponds to a larger GMR. The large variety of preparation conditions and in some cases the dominance of bulk scattering may in part explain the contradictory results.

In our opinion, the role of the interface in the GMR effect can only be evaluated if the following three conditions are fulfilled: (i) The electrical transport properties should be dominated by spin-dependent interface scattering instead of spin-dependent bulk scattering; (ii) the interface roughness should be quantitatively evaluated; (iii) the influence of the structural properties on the GMR should be analyzed in multilayers with a magnetoresistance larger than 20%, as proposed by Hood, Falicov, and Penn.[14]

In this paper we report on a detailed analysis of the correlation between the roughness at the interface and the GMR in polycrystalline Fe/Cr multilayers. The use of polycrystalline films grown by MBE techniques, makes it possible to draw conclusions independent of the crystallographic orientation, and allows a good comparison with the data reported for polycrystalline sputtered samples. The structural characteristics of the interface are influenced by the growth temperature (T_g) or by first covering the substrate with a Cr seed layer. The evaluation of the Fe/Cr interface is based on low-angle (LA) XRD measurements and the relevant electrical transport

data which are influenced by the roughening of the interfaces. We demonstrate that a Cr seed layer influences the superlattice structure, and therefore the GMR. Moreover, the growth temperature enables to optimize the superlattice structure and influences the electrical and magnetic properties. It is shown that the absence of compositional mixing or interdiffusion is necessary to obtain high GMR values. In some cases, atomic steps at the interfaces may favorably influence the GMR.

The superlattices were prepared in a Riber MBE deposition system (2×10^{-11} mbar base pressure) using electron-beam evaporation hearths, which were rate stabilized to within 1% by a homemade feedback control system[17] using Balzers quadrupole mass spectrometers (QMS). Additionally, integration of the QMS signal was used for automatic control of the shutters of the individual evaporation sources. In this way, a reproducible bilayer thickness throughout the whole superlattice is insured, as well as a constant Cr thickness over all superlattices. The Fe and Cr layers (starting material of 99.996% purity) were electron-beam evaporated in a pressure of 4×10^{-10} mbar at a rate of 1 Å/s on polycrystalline yttrium-stabilized zirconium oxide (YSZ) substrates (typically 5×5 mm^2). In order to minimize thickness inhomogeneities, the substrate was rotated at 60 rpm during the whole growth process. The surface roughness of the YSZ substrates was evaluated *ex situ* by atomic force microscopy (AFM). Typical rms values of the YSZ surface roughness were 5 Å on a 1-μm^2 area. After rinsing in isopropyl alcohol and drying in a dry N_2 flow, the substrate was annealed at 600°C in UHV conditions, during 15 min.

If no Cr seed layer was used, the growth of the superlattice began with an Fe layer (22 Å). In case a Cr seed layer was involved, we grew 20 Å of Cr on the YSZ substrate, while it was held at 50°C. Subsequently, the regular Fe/Cr superlattice was evaporated at its proper T_g, ranging from 0 to 400°C, in steps of 50°C. At every T_g value, we simultaneously evaporated a superlattice with and without a Cr buffer. In this way, we obtained a series of eighteen $[Fe(22)/Cr(13)]_{10}$ superlattices, grown at nine different growth temperatures, and consisting of ten bilayers with 22 Å of Fe and 13 Å of Cr.

Structural information about the superlattices was obtained from both LA- and HAXRD measurements using a Rigaku rotating anode diffractometer, at 4-kW power and with an x-ray wavelength of 1.542 Å (CuK_α). Three different experimental XRD setups have been used: (i) regular Bragg-Brentano (or θ-2θ) measurements at LA were used to determine the layering quality, the bilayer thickness Λ and the total thickness of the superlattice. From the HA spectra we obtained the crystallographic orientation(s) as well as the mean lattice constants normal to the sample plane; (ii) rocking curve or ω-scan measurements at HA providing information about the polar mosaic spread on the level of the atomic lattice spacing. The LA rocking curve data were taken to analyze the polar mosaic spread associated with the superlattice. The shape of the rocking curve is determined by the lateral length scales at which coherent interface roughness exists;[18] (iii) off-specular measurements in which the sample is tilted, so that the scattering vector is no longer perpendicular to the film plane. In this setup, a LA θ-2θ measurement enables to check whether the existing interface roughness is correlated throughout the superlattice.[19]

In this paper we will distinguish between two kinds of interface roughness: (i) compositional intermixing (or interdiffusion) and (ii) atomic steps, which may or may not be correlated throughout the superlattice. The electrical measurements were performed in an Oxford cryostat (1.5 up to 300 K) equipped with a 15-T magnet. Resistivities were determined using a standard four-probe Van der Pauw method. The magnetoresistance is defined as $\Delta\rho/\rho_s=(\rho_0-\rho_s)/\rho_s$, where ρ_0 is the resistivity in zero field and ρ_s the saturation resistivity in a parallel magnetic field H_s. All quoted resistivity values have been measured at 4.2 K.

In order to clarify the structural characteristics of the superlattices involved, we first discuss the HAXRD spectra. The bottom part of Fig. 1 shows a typical HAXRD spectrum of the Fe/Cr superlattices grown on YSZ. It corresponds clearly to a polycrystalline film, in which the different crystallographic orientations are visible (110 and 200 as the most intense). This is the expected growth mode for Fe/Cr on polycrystalline YSZ (at all chosen growth temperatures). We define a sample as being polycrystalline if the HA θ-2θ scan shows several FeCr orientations with the (110) orientations as the most intense. In that case, HA rocking curves around these peaks have a full width at half maximum (FWHM) larger than 20°, and are not longer well defined. If only one orientation of FeCr can be observed, and the associated rocking curve has a well-defined FWHM, the structure is textured with

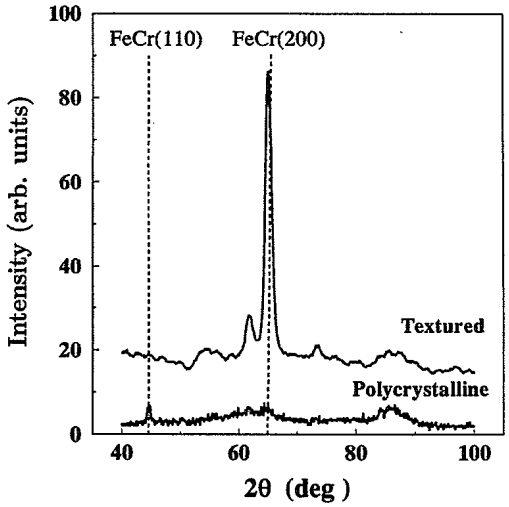

FIG. 1. High-angle XRD spectra of $[Fe(22)/Cr(13)]_{10}$ superlattices grown on a polycrystalline YSZ substrate. The bottom part shows a polycrystalline Fe/Cr superlattice, which is the usual growth mode. The upper part shows a (100) textured Fe/Cr superlattice, grown at a substrate temperature $T_g \geq 200$ °C on a YSZ substrate covered by a 20 Å seed layer of Cr. The curves are shifted vertically for clarity.

a preferential orientation in the observed direction. In the plane of the film, these superlattices have a random azimuthal distribution of the preferential orientation. The upper part of Fig. 1 shows the HA θ-2θ spectrum of a textured Fe/Cr superlattice grown at $T_g = 250\,^{\circ}\mathrm{C}$ on a Cr seed layer (50 °C). This (100) textured growth mode occurs only when a Cr seed layer is used and if T_g is of the order of 200 °C, or higher. From the structural point of view, a (100) preferential orientation is surprising for a textured bcc material, because the (110) plane is the most dense. However, Aldén *et al.*[20] calculated surface energies for both (100) and (110) bcc orientations and found a lower surface energy for the (100) plane. Similarly, Folkerts and Hakkens[21] observed (100) facets when Fe was grown on Ge(110), instead of the epitaxial (110) growth mode, which one expects from the structural point of view. The rocking curves of our (100) textured superlattices have a FWHM $\approx 5°$ to 10°, indicating that the angles over which the grains are tilted are quite large. Despite the differences observed in the HAXRD spectra between polycrystalline and textured films, the electrical transport properties do not reflect this difference, as will be shown later. This is not surprising since, in both cases, the crystallographic orientations are distributed randomly in the plane of the film.

Figure 2 shows the LAXRD spectra of the Fe/Cr superlattices grown at various substrate temperatures T_g. For the Fe/Cr multilayers grown on YSZ + Cr seed layer [Fig. 2(a)], the highest quality LAXRD spectrum is observed at a $T_g \approx 250\,^{\circ}\mathrm{C}$. At lower as well as higher T_g values, the LA spectra tend to loose superlattice peaks as well as finite-size peaks. The former indicates rougher interfaces; the latter can be seen as a loss of structural coherence between the top of the film and the film/substrate interface. The loss of specular intensity in the low and high-T_g regime should be attributed to different physical mechanisms. It was reported before that at lower T_g's the reduced surface mobility will introduce more steps in the growth of the superlattice,[22] while at higher T_g's, interdiffusion effects become more favorable, causing the rougher interfaces.[23] For the Fe/Cr layers grown without a Cr seed layer [Fig. 2(b)], the quality of the LAXRD spectra is optimized at a $T_g \approx 100\,^{\circ}\mathrm{C}$.

Comparing the LAXRD spectra in Figs. 2(a) and 2(b), it is clear that the superlattice peaks as well as the finite-size peaks are more pronounced when a Cr seed layer is used. Apparently, the Cr seed layer flattens and/or relaxes strain at the interface film/substrate, giving raise to a smoother growth of the superlattice. For both sets of samples [Figs. 2(a) and 2(b)] the finite-size peaks disappear, when layering quality is destroyed, indicating that worse layering automatically gives a rougher top surface. This means that the Cr layers with a thickness of 13 Å (grown at various T_g) within the Fe/Cr superlattice are not able to reestablish a smoother growth, in contrast to the underlying Cr seed layer of 20 Å (grown at 50 °C).

Figure 3 shows a typical rocking curve with 2θ fixed at the first-order superlattice peak of the LAXRD spectrum. The factor Q_{IF}, shown in the figure, will be defined later. The FWHM is 0.06°, which corresponds to the instrumental linewidth. The lower intensity at the left side of the maximum is due to the limited sample size. The steeper the decay of the intensity away from the central peak, the longer the lateral correlation length of the interface roughness contributing to the background.[20] This makes it possible to distinguish interdiffusion (small correlation lengths) from atomic steps (larger correlation lengths). The absence of an additional structure, away from the central peak, in the LA rocking curve, may indicate that (i) the interface roughness is not coherent throughout the whole superlattice or (ii) the roughness is coherent but is spread homogeneously over all lateral length scales. Away from the central peak in Fig. 3 one observes a homogeneous spread of the background intensity, thus indicating that the interface roughness is not correlated throughout the superlattice, or if correlated, is

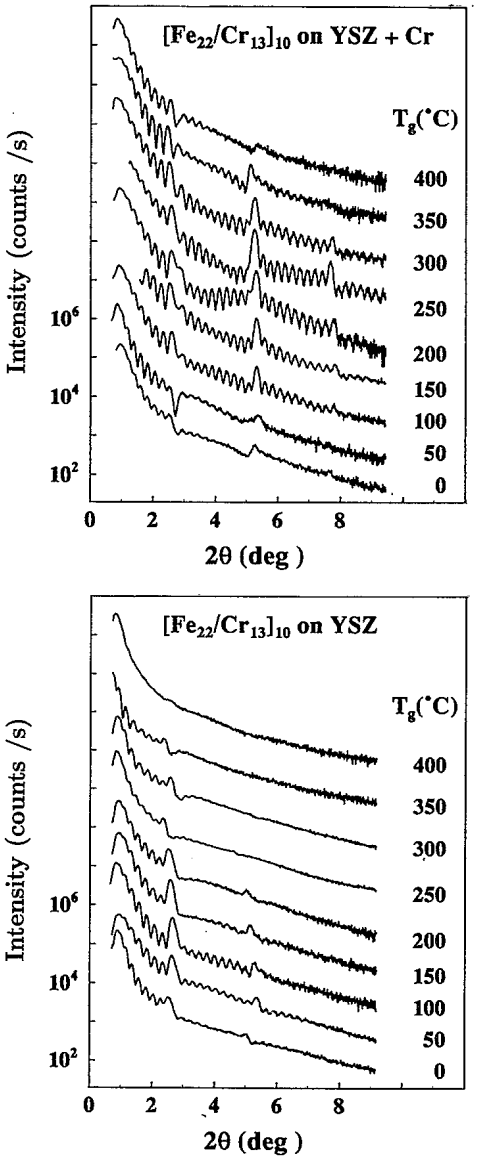

FIG. 2. Low-angle XRD spectra for $[Fe(22)/Cr(13)]_{10}$ superlattices both with (a) and without (b) a Cr seed layer, as function of the substrate temperature T_g. Curves at different T_g are shifted vertically for clarity.

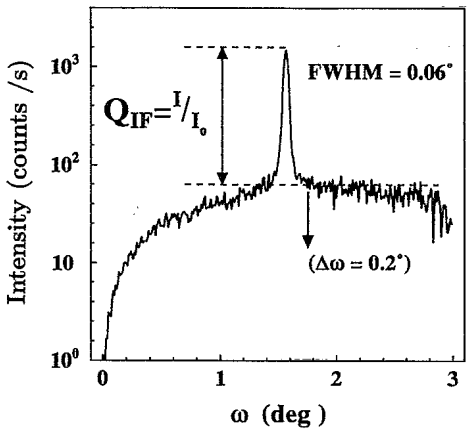

FIG. 3. Rocking curve (ω-scan) around the first-order superlattice peak at low angles. The interface quality factor Q_{IF} is defined as the ratio of peak (I) and background (I_0) intensity. $\Delta\omega=0.2°$ defines the offset in θ that we take into account in the off-specular measurements.

homogeneously distributed over all lateral length scales.

To check the origin of the background intensity, i.e., the nature of the interface roughness, we performed off-specular θ-2θ measurements at LA, with an offset in the θ angle ($\Delta\omega$) of 0.2 °. In this way, we are out of the Bragg condition for the superlattice period, but in the Bragg condition for the (correlated) roughness. Figure 4 shows the specular as well as the off-specular LAXRD spectra of three identical Fe/Cr superlattices grown on YSZ + Cr seed layer at $T_g=50$, 200, and 400 °C. Comparing these results with data from literature,[22] one observes little evidence for any correlation, indicating mainly diffuse scattering from the interfaces. This means that most of the intensity aside from the central peak should be attributed to uncorrelated roughness.

In order to quantify the layering quality using the LAXRD spectra, we evaluate the signal-to-background ratio of the rocking curve at the first superlattice peak in the LA spectrum. As mentioned before, the relative background intensities in such a plot are correlated to the interface roughness. Therefore, we define an interface quality factor Q_{IF} as the ratio of the scattered intensity (I) from the coherent interfaces, over the overall background intensity (I_0): i.e., $Q_{IF}=I/I_0$, as displayed in Fig. 3. This interface quality factor Q_{IF} is plotted against growth temperature in Figs. 5(a) and 5(b) for two sets of Fe/Cr superlattices. The interface quality evaluated this way, is optimized at $T_g\approx250$ °C when a Cr seed layer is used and at $T_g\approx100$ °C for the Fe/Cr superlattices directly grown on the bare YSZ substrate. This is in agreement with the qualitative analysis of the data shown in Figs. 2(a) and 2(b). This means that indeed, what we visually observed as being the best quality LA spectrum, can be quantitatively evaluated by the use of the interface quality factor Q_{IF}.

The detailed evaluation of the XRD spectra clearly demonstrates the possibility to optimize the amount of interface roughness by changing the growth temperature and/or the use of a Cr seed layer. The crucial question, however, is whether we can observe a correlation between interface roughness and the electrical transport properties in these polycrystalline superlattices. Can the GMR effect be linked to the interface roughness, and is in polycrystalline Fe/Cr the resistivity mainly governed by interface effects? If interface scattering, instead of bulk scattering, dominates, we should expect a minimum resis-

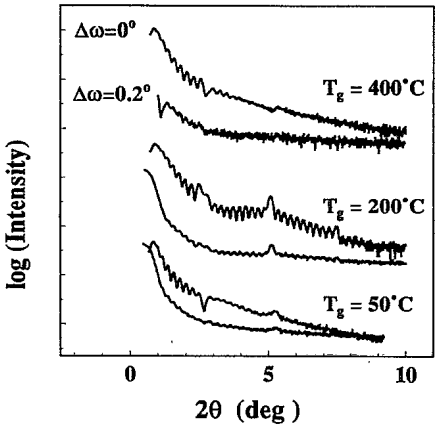

FIG. 4. Low-angle XRD spectra (θ-2θ) at three different growth temperatures T_g. The curves labeled with $\Delta\omega=0°$ are θ-2θ measurements in the specular setup with the scattering vector perpendicular to the sample plane. The curves labeled with $\Delta\omega=0.2°$ are so called off-axis θ-2θ measurements with the scattering vector turned over 0.2° with respect to the surface normal.

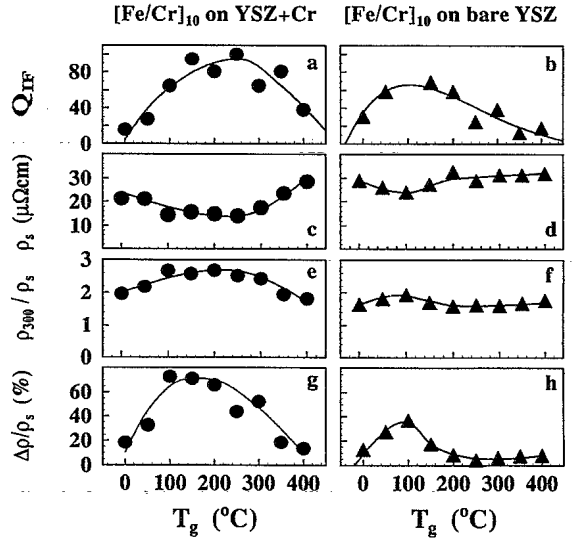

FIG. 5. The data shown in (a), (c), (e), and (g) are related to the [Fe(22)/Cr(13)]$_{10}$ superlattices grown on a YSZ substrate covered by a Cr seed layer. The same parameters are shown in (b), (d), (f), and (h) when no Cr seed layer is used. The following parameters are shown as function of the substrate temperature T_g: interface quality factor Q_{IF} (a) and (b); saturation resistivity ρ_s at 4.2 K (c) and (d); residual resistance ratio ρ_{300}/ρ_s (e) and (f), and the GMR $\Delta\rho/\rho_s$ (g) and (h).

tivity around the growth temperature where the interface roughness is the smallest. We will concentrate on the saturation resistivity ρ_s in order to eliminate the magnetoresistive contribution due to the antiferromagnetic ordering in a zero field. In this way, ρ_s is determined by all kinds of crystal imperfections (impurities, grain boundaries, interface roughness), and is therefore a reflection of the crystalline quality. If ρ_s shows a dependence on T_g, consistent with the interface roughening, we may conclude that the resistivity is mainly determined by interface roughness instead of bulk scattering. Figures 5(c) and 5(d) show ρ_s as function of T_g for Fe/Cr superlattices grown on YSZ, with and without a Cr seed layer. The superlattices with a seed layer [Fig. 5(c)] have a lower ρ_s at all growth temperatures, compared to the films on bare YSZ. This is consistent with the higher LAXRD quality factor Q_{IF} for this set of samples [Fig. 5(a)]. When a Cr buffer is used, $\rho_s(T_g)$ shows a minimum at 250 °C [Fig. 5(c)]. For the superlattices directly grown on YSZ, ρ_s has its minimum value at 100 °C [Fig. 5(d)]. Comparing this with the structural interface characteristics of Figs. 5(a) and 5(b), we can conclude that indeed the smaller interface roughness, the lower the saturation resistivity at 4.2 K. For both sets of samples, one observes changes in ρ_s of the order of 50–100 %, when the interface structure is modified by varying T_g between 0 and 400 °C. Therefore ρ_s is indeed a good parameter for evaluating the crystalline perfection of the film, which is in this case dominated by the interface roughness.

Figures 5(e) and 5(f) show the residual resistivity ratio ρ_{300}/ρ_s, with ρ_{300} the resistivity at room temperature in zero field. This ratio is a measure for the amount of scattering still present at low temperature, and thus a kind of quality factor, evaluating the superlattice from the structural point of view. We clearly observe a maximum of ρ_{300}/ρ_s at $T_g \approx 250$ °C and at $T_g \approx 100$ °C for Fe/Cr superlattices on YSZ+Cr and bare YSZ substrates, respectively. This is fully consistent with the other structural and resistive data discussed so far: a better interface structure corresponds to a lower ρ_s and a higher ρ_{300}/ρ_s.

Finally, how is the structural quality of the interface influencing the GMR values of the FeCr superlattices? Figures 5(g) and 5(h) show the GMR as a function of the growth temperature T_g. The highest GMR values are clearly present in Fe/Cr superlattices in which the Cr seed layer improves the layering quality. A GMR of 70% MR is obtained when T_g is optimized. The maximum GMR, for both sets of samples, occurs at those growth temperatures where Q_{IF} shows a maximum, i.e., when the best layering quality is realized.

It should be noted that the behavior of $\Delta\rho = \rho_0 - \rho_s$ as function of T_g is similar to that of $\Delta\rho/\rho_s$. This shows that the GMR is governed by the spin-dependent scattering $\Delta\rho$, rather than by the nonmagnetoresistive ρ_s.

Analyzing the peak positions in Fig. 5, for the Fe/Cr superlattices grown on a Cr seed layer, we found a coincidence of the extrema of Q_{IF}, ρ_s, and ρ_{300}/ρ_s. However, there is some evidence that the maximum amplitude of the GMR [Fig. 5(g)] is shifted slightly towards lower T_g values compared to the other parameters. This indicates that a small amount of steps at the interface can enhance the GMR.

Comparing the different plots in Fig. 5, we observe different optimal T_g values whether the Fe/Cr superlattice was grown on a Cr seed layer ($T_g \approx 200$ °C) or on the bare substrate ($T_g \approx 100$ °C). Why is interdiffusion degrading the interfaces already at a lower T_g when no Cr seed layer is used? It is well known that grain boundaries are good channels via which interdiffusion takes place.[24] Therefore we checked the grain-boundary density on these polycrystalline Fe/Cr superlattices by means of atomic force microscopy (AFM). For the superlattices grown at $T_g = 150$ °C, the surfaces showed a mean lateral grain diameter of 200 Å without a Cr seed layer and 1000 Å in the case a Cr seed layer is used. This proves that the density of grain boundaries is the lowest when a Cr buffer is used. Therefore, at $T_g = 150$ °C, the superlattices grown on a Cr seed layer will be less affected by interdiffusion than those grown on the bare YSZ substrate.

Finally, it should be noted that the change in the crystallographic structure from polycrystalline to (100) textured when T_g is increased (for the superlattices on a Cr seed layer) does not influence the interface structure or the electrical transport properties. Neither the interface quality nor the transport properties show any discontinuity between $T_g = 150$ °C and $T_g = 200$ °C. This is an additional proof that the transport properties of these polycrystalline Fe/Cr superlattices are not governed by bulk scattering.

The relation we found between the interface structure and the GMR effect is in qualitative agreement with previous experiments on sputtered Fe/Cr superlattices by Takanashi *et al.*,[9] Joo *et al.*,[12] and Rensing, Payne, and Clemens[11] although the transport properties of these layers are governed by bulk scattering. Fullerton *et al.*[13] found an increase of the GMR with increasing interface roughness. This seems to be contradictory to our results. However, they attribute the changes in the XRD spectra to interface roughness rather than interdiffusion, which is to some extent in agreement with our results. But again the amplitudes of the GMR values are rather low and bulk scattering may be dominant.

In conclusion, we investigated the correlation between interface properties and the amplitude of the GMR of polycrystalline Fe/Cr superlattices grown by MBE. We proved that the transport properties are governed by interface scattering rather than by scattering at intralayer defects. The quantitative evaluation of the interface structure is based on LAXRD rocking curves. We found that both interdiffusion and important interface roughness reduce the GMR amplitude.

This work is financially supported by the Belgian Concerted Action (GOA) and Interuniversity Attraction Poles (IUAP) programs. R.S., C.D.P., and G.V. are supported by, respectively, the Human Capital and Mobility Program of the European Community, the Research Council of the Katholieke Universiteit Leuven, and the Belgian Interuniversity Institute for Nuclear Sciences.

[1]P. Grünberg, R. Schreiber, Y. Pang, M. B. Brodsky, and H. Sowers, Phys. Rev. Lett. **57**, 2442 (1986).
[2]C. Carbone and S. F. Alvorado, Phys. Rev. B **36**, 2433 (1987).
[3]M. N. Baibich, J. M. Broto, A. Fert, F. Nguyen Van Dau, F. Petroff, P. Etienne, G. Creuzet, A. Friederich, and J. Chazelas, Phys. Rev. Lett. **61**, 2472 (1988).
[4]F. Petroff, A. Barthelemy, A. Hamzic, A. Fert, P. Etienne, S. Lequien, and G. Creuzet, J. Magn. Magn. Mater. **93**, 95 (1991).
[5]S. S. P. Parkin, Phys. Rev. Lett. **71**, 1641 (1993); K. Takanashi, Y. Obi, N. Tsuda, and H. Fujimore, J. Phys. Soc. Jpn. **61**, 4148 (1992).
[6]J. Unguris, R. J. Celotta, and D. T. Pierce, Phys. Rev. Lett. **67**, 140 (1991).
[7]S. S. P. Parkin, Phys. Rev. Lett. **67**, 3598 (1991).
[8]C. D. Potter, R. Schad, P. Beliën, G. Verbanck, V. V. Moshchalkov, and Y. Bruynseraede, Phys. Rev. B **49**, 16 055 (1994).
[9]K. Takanashi, Y. Obi, Y. Mitani, and H. Fujimore, J. Phys. Soc. Jpn. **61**, 1169 (1992).
[10]S. S. Parkin and B. R. York, Appl. Phys. Lett. **62**, 1842 (1993).
[11]N. M. Rensing, A. P. Payne, and B. M. Clemens, J. Magn. Magn. Mater. **121**, 436 (1993).
[12]S. Joo, Y. Obi, K. Takanashi, and H. Fujimori, J. Magn. Magn. Mater. **104-107**, 1753 (1992).
[13]E. E. Fullerton, D. M. Kelly, J. Guimpel, I. K. Schuller, and Y. Bruynseraede, Phys. Rev. Lett. **68**, 859 (1992).
[14]R. Q. Hood, L. M. Falicov, and D. R. Penn, Phys. Rev. B **49**, 368 (1994).
[15]Y. Asano, A. Oguria, and S. Maekawa, Phys. Rev. B **48**, 6192 (1993).
[16]J. Barnas, A. Fuss, R. E. Camley, P. Grüberg, and W. Zinn, Phys. Rev. B **42**, 8110 (1990).
[17]W. Sevenhans, J.-P. Locquet, and Y. Bruynseraede, Rev. Sci. Instrum. **57**, 937 (1986).
[18]D. E. Savage, N. Schimke, Y.-H. Phang, and M. G. Lagally, J. Appl. Phys. **71**, 3283 (1992).
[19]E. E. Fullerton, J. Pearson, C. H. Sowers, S. Bader, X. Z. Wu, and S. K. Sinha, Phys. Rev. B **48**, 17 432 (1993).
[20]M. Aldén, S. Mirbt, H. L. Skriver, N. M. Rosengaard, and B. Johansson, Phys. Rev. B **46**, 6303 (1992).
[21]W. Folkerts and F. Hakkens, J. Appl. Phys. **73**, 3922 (1993).
[22]J. A. Stroscio, D. T. Pierce, and R. A. Dragoset, Phys. Rev. Lett. **70**, 3615 (1993).
[23]J. Korecki and U. Gradmann, Phys. Rev. Lett. **55**, 2491 (1985).
[24]A. G. Guy, *Introduction to Materials Science* (McGraw-Hill, Tokyo, 1972).